2 Duffy, J., 1990, "The Fallacy of Modern Hybrid Control Theory that is Based Upon 'Orthogonal Complements' of Twists and Wrench Spaces," (editorial) *Journal of Robotic Systems*, Vol. 7, No. 2, pp. 139–144.
3 Erdman, A., 1992, *The First 40 Years of Modern Kinematics*, John Wiley and Sons.
4 Hamilton, W. R., 1969, *Elements of Quarternions*, (reprinted) Chelsea Press.
5 Kazerounian, K., and Rastegar, J., 1992, "Object Norms: A Class of Coordinate and Metric Independent Norms for Displacements," *Proc. of the 1992 ASME Design Technical Conferences, Flexible Mechanisms, Dynamics, and Analysis*, DE-Vol. 47, pp. 271–275, September.
6 McCarthy, J. M., 1983, "Planar and Spherical Rigid Motion as Special Cases of Spherical and 3-Spherical Motion," ASME JOURNAL OF MECHANISMS, TRANSMISSIONS, AND AUTOMATION IN DESIGN, Vol. 105, September, pp. 569–575.
7 McCarthy, J. M., 1986, "On the Relation Between Kinematic Mappings of Planar and Spherical Displacements," ASME *Journal of Applied Mechanics*, Vol. 53, June, pp. 457–459.
8 McCarthy, J. M., 1990, *An Introduction to Theoretical Kinematics*, MIT Press.
9 Ravani, B., and Roth, B., 1983, "Motion Synthesis Using Kinematic Mappings," ASME JOURNAL OF MECHANISMS, TRANSMISSIONS, AND AUTOMATION IN DESIGN, Vol. 105, September, pp. 460–467.
10 Suh, C. H., and Radcliffe, C. W., 1978, *Kinematics and Mechanism Design*, John Wiley and Sons.

Quadri-directional Air Thrusters for Free-floating Robot Applications

N. Batsios,[1] M. Annapragada,[1] and Sunil Kumar Agrawal[2]

This paper describes the operational theory and design of a quadri-directional air thruster ("quad") for propulsion of the free-floating robot of Ohio University. In this design, the air is drawn from a central air tank and routed to four nozzles of a quad thruster via a pressure regulator, a distribution manifold, four solenoid valves, and a quad manifold. The pressure regulator is controlled by a d.c. servomotor and the solenoid valves are turned on/off using the digital output ports of the computer. The performance characteristics of this quad thruster were determined experimentally. The experimental measurement of the thrust as a function of the regulated pressure shows a good match with the data predicted by the supporting theory.

1 Introduction

Over the last two decades, a number of analytical and experimental studies have been reported on free-floating space robots [3], [1], [5]. In an effort to understand robotic assemblies in a zero gravity space environment, a free-floating robot facility is being developed at Ohio University with a dual-arm planar robot equipped with thrusters. Regulated supply of air floats the robot on a granite surface. Two quad-thrusters are mounted on the base to propel the robot with servomotor controlled pressure regulators to direct the air to the nozzles of the quad thruster.

Even though a number of aspects of the analytical work and experimental setup could be of interest to the reader, this paper addresses the aspects of design of the quadridirectional thruster. This paper is organized in the following way. The operational theory of the air thruster is outlined in Section 2. The experiment setup and the results are described in Section 3. These are followed by conclusions.

2 Operational Theory

Consider a reservoir (r) that discharges air through the outlet (o) of a converging nozzle into the atmosphere. For ideal gases, under the condition of isentropic flow, using continuity and conservation of energy [4], it can be shown that the ratio of the outlet and reservoir pressures is:

$$\frac{P_0}{P_r} = \frac{1}{\left[1 + \frac{\gamma - 1}{2} M^2\right]^{\gamma/\gamma - 1}} \tag{1}$$

where $P_0 = P_{atm}$, $\gamma = 1.4$ for air, and M is the Mach number of air flow at the outlet. The ratio of the outlet temperature and reservoir temperature is given by the following equation:

$$\frac{T_0}{T_r} = \frac{1}{1 + \frac{\gamma - 1}{2} M^2} \tag{2}$$

The velocity of air V_o at the outlet is $V_o = M\sqrt{\gamma R T_0}$ and the density ratio is given by

$$\frac{\rho_0}{\rho_r} = \left[\frac{T_0}{T_r}\right]^{1/\gamma - 1} \tag{3}$$

The thrust, F, generated by the air flow is

$$F = \frac{P_0 A_0 V_0^2}{R T_0} \tag{4}$$

Once the reservoir pressure is measured, the Mach number of the air flow can be computed from Eq. (1), T_0 from Eq. (2), and the thrust from Eq. (4).

The outlet velocity of the air flow from a converging nozzle never exceeds the velocity of sound. When the Mach number of air flow at the outlet becomes one, the flow is said to be choked. On substituting $M = 1$ in the above equations, we get:

$$\frac{P_0}{P_r} = \left[\frac{2}{\gamma + 1}\right]^{\gamma/\gamma - 1}, \quad \frac{T_0}{T_r} = \frac{2}{\gamma + 1}, \quad \frac{\rho_0}{\rho_r} = \left[\frac{2}{\gamma + 1}\right]^{1/\gamma - 1} \tag{5}$$

The thrust, F, generated by the air flow is

$$F = (\rho_0 V_0 A_0) V_0 = \frac{P_r A_0 V_0^2}{R T_r} \left[\frac{2}{\gamma + 1}\right]^{\gamma/\gamma - 1} \tag{6}$$

where A_0 is the area of the outlet nozzle, V_0 is the outlet velocity of the air equal to the speed of sound, and R is the universal gas constant.

Mark's Handbook [2] modifies the volumetric flow rate of air through the outlet computed in the last two paragraphs in the following way:

$$\dot{Q}_{actual} = CEY\dot{Q}_{ideal} \tag{7}$$

where C is a coefficient based on Reynold's number of the fluid flow, E is dependent on the ratio of inlet and outlet areas of the nozzle, and Y is a function of the ratio of reservoir to outlet pressure and ratio of the inlet and outlet areas of the nozzle. Hence, the outlet thrust of the nozzle according to Mark's Handbook scales the theoretical thrust by the constant CEY.

A plot of the outlet velocity as a function of reservoir pressure is shown in Fig. 1. From this plot, we observe that the velocity of the outlet air becomes a constant once the reservoir achieves a critical pressure for the choked flow. Figure 2 shows a plot of the thrust as a function of the reservoir pressure based on the operational theory for an outlet diameter of the nozzle.

[1] Graduate Students.
[2] Associate Professor, Mechanical Systems Laboratory, Department of Mechanical Engineering, Ohio University, Athens, OH 45701.
Contributed by the Mechanisms Committee for publication in the JOURNAL OF MECHANICAL DESIGN. Manuscript received Feb. 1994; revised May 1995. Technical Editor: B. Ravani.

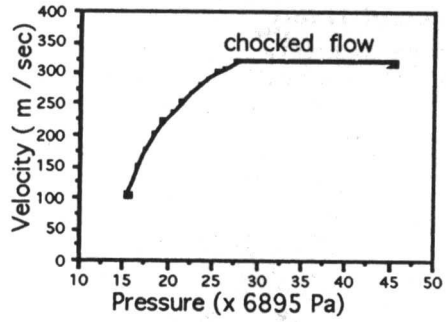

Fig. 1 A plot of the outlet velocity as a function of the reservoir pressure based on operational theory

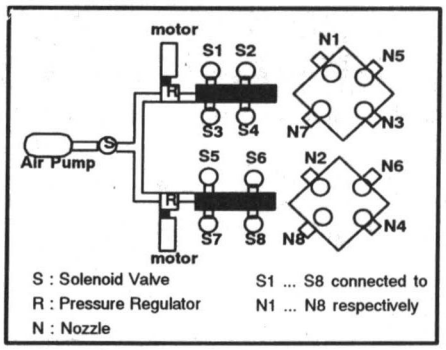

Fig. 3 A schematic of the mechanical circuit of the air thrusters

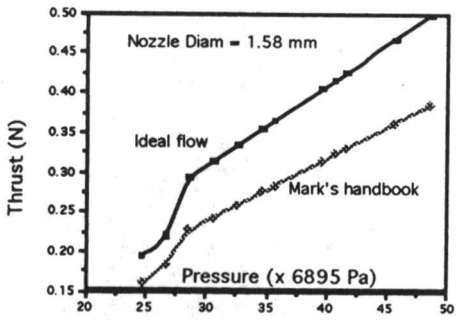

Fig. 2 A comparison of the thrust as a function of the reservoir pressure based on operational theory for an outlet diameter of the nozzle

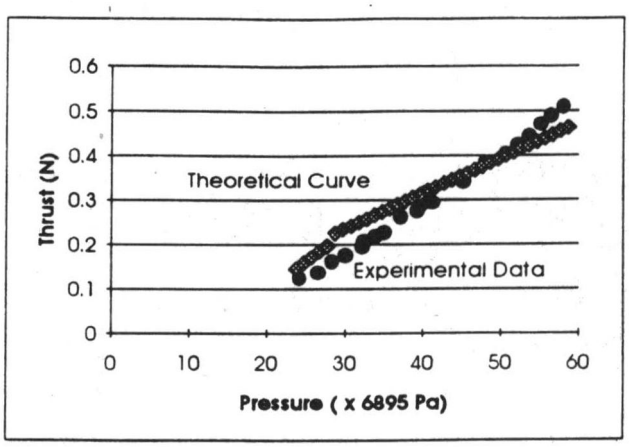

Fig. 4 Output thrust from experiment measurements and operational theory using Mark's handbook for nozzle diameter of 1.58 mm

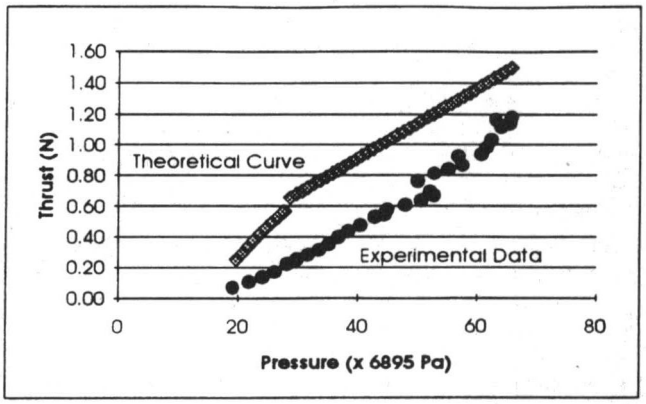

Fig. 5 Output thrust from experiment measurement and operational theory using Mark's handbook for nozzle diameter of 3.975 mm

3 Experiment Setup and Results

Two quad thrusters, with identical designs, were tested in the laboratory. A block diagram of the mechanical circuit is shown in Fig. 3. The details of a single quad thruster are as follows. A pressure regulator, controlled by a d.c. servomotor, modulates the input air pressure supplied by the tank. The air then flows into a distribution manifold with four exit holes. The air flow through each hole is controlled by a solenoid valve. The air from these exits is routed to four inlets of a quad manifold. Each inlet of the quad manifold is connected to an outlet, on which a nozzle of a desired exit diameter is screwed on.

The two pressure regulators are controlled by two servomotors via a PC 386 using a motion control system. A calibration is performed between the angular displacement of the servomotor and the output pressure of the regulator. It was found that the relationship between output pressure and the servomotor displacement was linear. The eight solenoid valves (four solenoid valves per thruster) are controlled by digital output ports of the PC 386. The thrust was measured by placing the quad on a balance with an accuracy of a tenth of a gram. As the air escaped out of a nozzle, the balance provided a reading of the thrust.

Figures 4 and 5 show experimentally measured output thrust as a function of the reservoir pressure for two outlet diameters of the nozzle. The figures also overlay the corresponding data predicted from the operational theory given in Mark's handbook. From these figures, we conclude that there is a good match between the experiment and theoretical data for the nozzle of output diameter 1.58 mm. Also, the experimentally obtained thrust data is a linearly varying function of pressure. This makes it convenient for development of control algorithms. However, for the nozzle of diameter 3.975 mm, there is a difference between the experimental and theoretical characteristics. Perhaps, this is attributed to the accuracy and smoothness of machining of the nozzle. However, the thrust is still a linear function of the pressure.

4 Conclusions

In this paper, we described the operational theory and a working design of a quadridirectional air thruster for the purposes of propulsion of free-floating robots. We showed that the performance characteristics of this design show a reasonably good match with the predictions of the operational theory. We feel that this design is worth reporting to the readers because of its simplicity and low cost. Further, the authors believe that this design has great potential for conducting benchmark laboratory experiments for future space robotics applications.

5 Acknowledgments

The support of NSF grant CMS 9402435 is gratefully acknowledged.

References

1 Agrawal, S. K., Chen, M. Y., and Annapragada, M., 1995, "Modeling and Simulation of Assembly in a Free-floating Environment by a Free-floating Robot," ASME JOURNAL OF MECHANICAL DESIGN.

2 Avallone, E. A., and Braumeister, T., 1986, *Mark's Standard Handbook for Mechanical Engineers*, McGraw Hill Book Company.

3 Schneider, S. A., and Cannon, R. H., 1992, "Object Impedance Control for Cooperative Manipulation: Theory and Experimental Results," *IEEE Transactions on Robotics and Automation*, Vol. 8, June, pp. 383–394.

4 White, F. M., 1986, *Fluid Mechanics*, McGraw Hill Book Company.

5 Xu, Y., and Kanade, T., 1993, *Space Robotics: Dynamics and Control*, Kluwer Academic Publishers.

A New Family of Parameterized Polynomials for Cam Motion Synthesis

Q. Yu[1] and H. P. Lee[2]

Introduction

The traditional method to design a polynomial curve uses a set of boundary conditions to determine the coefficients of the polynomial. One distinct polynomial curve is obtained for each set of constraints. As there is no direct relation between the constraints and the kinematic features such as the maximum velocity V_m and the maximum acceleration A_m of the polynomial curve, the rules as how to specify the constraints largely depend on the experience of designers. To improve and simplify the traditional design method, a family of parameterized polynomials is introduced in this paper. It consists of four parameterized polynomials and each of them has one parameter and different boundary continuity. Their kinematic relations between the kinematic features, such as V_m and A_m, and the parameter are known. So, a designer can control the continuity of the curve by selecting different parameterized polynomials in the family and vary the kinematic feature by changing the parameter according to the known kinematic relations. Many well-known important motion curves are found to exhibit exact or very close kinematic features with the parameterized polynomial curves. Moreover, linear combinations of the independent portions of the polynomials in the family can further extend the flexibility of motion curves.

The design of the dwell-rise-dwell (DRD) curve is used as an example in this paper. The acceleration curve is assumed to be antisymmetrical about the midspan of the rise interval because the violation of antisymmetric features of the motion curve will lead to an increase in the maximum acceleration. The follower displacement expressed in this paper is a normalized quantity.

The Proposed Family of Parameterized Polynomials

It is known (Chen, 1982) that to maintain the antisymmetric property of the acceleration of a normalized polynomial, the displacement is in the following form

$$S(\theta) = \sum_{i=j}^{k} C_i \theta^i \qquad (1)$$

where j and k are positive integers. The variable θ is defined for the interval from 0 to 1. The normalized displacement S is equal to 1 at the end of the interval.

To keep the antisymmetry property of the curve the following constraints are adopted: (a) at the end of the rise interval, $S(1) = 1$; (b) the order of continuity at the point of $\theta = 1$ must be $j - 1$; (c) the acceleration equals zero at the midpoint of the rise interval. Therefore, the total number of constraints is equal to $j + 1$. A polynomial of form (1) with $j + 1$ terms will be sufficient to satisfy all the constraints. To obtain a parameterized polynomial with one additional coefficient in (1) more than the number of given constraints, the total number of coefficients or terms in (1) is $k - j + 1 = j + 2$. Therefore, the value of k in (1) for a parameterized polynomial is given by $k = 2j + 1$. To satisfy all the $j + 1$ given constraints, similar to the traditional method, $j + 1$ linear equations of coefficients can be obtained. Since there is one more coefficient compared to the number of equations, every coefficient can be expressed as a linear function of a parameter, resulting in parameterized polynomials.

Four parameterized polynomials shown in Table 1 are obtained by setting the integer k in (1) to be 5, 7, 9, and 11, respectively. Higher order polynomials can be obtained in the same manner. The symbol $S^{(4)}(\theta)$ is the 4th derivative of S with respect to θ. Instead of expressing every coefficient as a linear function of a parameter the polynomials are rearranged to consist of a parameter-independent polynomial and a parameter-dependent polynomial so that the effect of varying the parameter β can be easily examined. The subscript of the symbol in Table 1 represents the highest order of the polynomial.

The Kinematic Features of the Family

Since a parameterized polynomial in Table 1 has only one parameter, the relations between some kinematic features of the parameterized polynomial and the parameter can be shown. The kinematic features chosen to make the investigation of these relations are:

(1) the maximum velocity, V_m;
(2) the maximum acceleration, A_m;
(3) the integral of acceleration square, $D = \int_0^1 A^2 d\theta$;
(4) the integral of velocity square, $E = \int_0^1 V^2 d\theta$.

Figures 1(a) to (d) show changes of these kinematic quantities with β. The range of β in these figures is set to meet the general requirements for engineering designs. The special points corresponding to the normalized 3-4-5 and 4-5-6-7 polynomials are indicated in the figure. A 3-4-5 polynomial is a curve of S_5 or S_7 with $\beta = 1$. A 4-5-6-7 polynomial is a curve of S_7 or S_9 with $\beta = 2$. The relations shown in Fig. 1 provide a large number of choices of motion curves for the different requirements on boundary continuity and kinematic features.

Table 1 The proposed parameterized polynomials

Continuity	Symbol	Expressions of the Family θ [0, 1]
Velocity	$S_5(\theta, \beta)$	$3\theta^2-2\theta^3-(3\theta^2-12\theta^3+15\theta^4-6\theta^5)\beta$
Acceleration	$S_7(\theta, \beta)$	$20\theta^3-65\theta^4+96\theta^5-70\theta^6+20\theta^7$ $-(10\theta^3-50\theta^4+90\theta^5-70\theta^6+20\theta^7)\beta$
Jerk	$S_9(\theta, \beta)$	$105\theta^4-504\theta^5+1050\theta^6-1140\theta^7+630\theta^8-140\theta^9$ $-(35\theta^4-210\theta^5+490\theta^6-560\theta^7+315\theta^8-70\theta^9)\beta$
$S^{(4)}(\theta)$	$S_{11}(\theta, \beta)$	$504\theta^5-3066\theta^6+8100\theta^7-11655\theta^8+9520\theta^9-4158\theta^{10}+756\theta^{11}$ $-(126\theta^5-882\theta^6+2520\theta^7-3780\theta^8+3150\theta^9-1386\theta^{10}+252\theta^{11})\beta$

[1] Research Student.

[2] Senior Lecturer, Assoc. Member, ASME, Department of Mechanical and Production Engineering, National University of Singapore, 10 Kent Ridge Crescent, Singapore 0511

Contributed by the Mechanisms Committee for publication in the JOURNAL OF MECHANICAL DESIGN. Manuscript received June 1994; revised April 1995. Associate Technical Editor: J. Anseles.